SCALING EFFECTS ON THE EFFICIENCY OF MICRO-SCALE GAS TURBINES

Andrew P. Camacho[1*], I. Wang[1], J. Jaworski[1], J.M. Protz[1]
[1]Department of Mechanical Engineering and Materials Science, Duke University, Durham, U.S.A.
*Presenting Author: apc6@duke.edu

Abstract: A fluid dynamic analysis of an adiabatic micro gas turbine is presented to demonstrate the theoretical dependence of efficiency, entropic losses, and power density on turbine size. The loss mechanisms associated with the viscous boundary layer, trailing edge wake mixing, and tip leakage are modeled to determine turbine efficiency across a range of diameter, rotor speed, reaction, and stage count. The results demonstrate quantitatively how viscous losses and losses associated with manufacturing tolerances and feature resolution become increasingly dominant as turbine size decreases. The results identify a peak power density at a critical turbine diameter, below which the benefits associated with the squared-cubed law are overcome by increasingly dominant viscous losses.

Keywords: turbomachinery, microturbine, losses, efficiency

INTRODUCTION

The present work addresses turbomachinery losses arising from insufficient tip speed, boundary layer formation and growth, trailing edge wake mixing, and tip clearance and how these losses vary with scale. At small sizes and low Reynolds numbers, viscous losses from boundary layer growth are exceptionally important. Tip leakage and trailing edge mixing losses are also more significant at smaller sizes due to the poorer feature resolution of the geometry dictated by manufacturing and stress constraints when compared to conventionally sized machines [1]. In addition, because the optimal tip speed of turbines does not scale down with size, extremely high values of angular velocity are required for microturbines, which are often difficult to achieve reliably. If the appropriate rotor speed cannot be reached, non-utilized kinetic energy will remain in the exit flow, lowering total-to-static efficiency.

Combining the methods presented in Denton [2] and Greitzer [3], the entropic loss mechanisms are explained and modeled from theoretical first-principles and empirical boundary layer data. The objective is to create an array of design charts that enables engineers to roughly estimate the performance and efficiency of variously sized turbines over a range of RPM, reaction, and stage count. An example is shown in Fig. 1. The results also quantitatively demonstrate how power density scales with turbine size.

Turbine Modeling

The turbines in this analysis were modeled as axial turbines that are scaled geometrically based on the outer diameter while retaining the same mass flux, a total-to-static pressure ratio of P_{t1}/P_e=1.85, and a turbine inlet total temperature of T_{t1}=1400 K. Four different turbines varieties were analyzed: single-stage impulse, single-stage 50% reaction, two-stage impulse, and three-stage impulse. All impulse turbine designs were designed as velocity-compounded Curtis turbines where the pressure drop across occurs strictly in the nozzle guide vanes, and subsequent stator rows only redirect the flow.

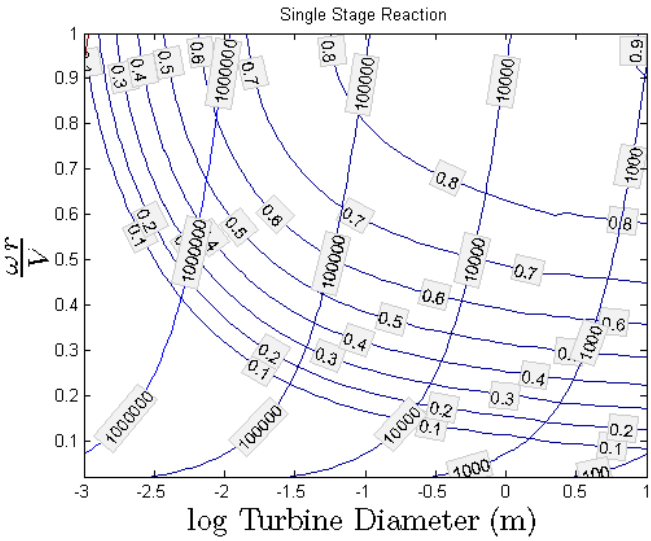

Fig. 1: Total-to-static efficiency of a single stage 50% reaction turbine as a function of the velocity ratio, diameter, and RPM.

LOSS MECHANISMS

Loss Accounting

For internal flow through turbomachines, a common metric of loss is entropy creation because its value does not depend on the reference frame from which it is viewed. As stated in Greitzer [3], in a non-ideal flow with total pressure drop, the amount of work required to bring an irreversible flow process back to its initial state is related to entropy creation by

$$w_{rev} = T_t \Delta s \quad (1)$$

By quantifying the entropy creation due to the different loss mechanisms, the amount of lost work can be computed and used to estimate efficiency.

Flow Characterization

For all three loss mechanisms modeled, various parameters of the flow over the blades must be known. For example, the velocity distribution must be estimated over each blade in order to approximate various boundary layer parameters such as the displacement and momentum thickness.

Following Denton [2], the difference in velocities on the blade surfaces can be roughly estimated by assuming that the blade loading is constant. By then using the definition of circulation and setting its value to zero for the non-lifting flow channel, the velocity difference between the suction and pressure side is

$$V_S - V_P \approx \frac{p}{c} u(\tan\alpha_2 - \tan\alpha_1) \qquad (2)$$

where p is the blade pitch, C is the chord, and u is the axial velocity. The relative velocity V_r at the trailing edge as determined from 1-D calculations is used as the mean value of the suction and pressure surface velocities. This approach results in idealized velocity distributions as shown in Fig. 2, which allow one to

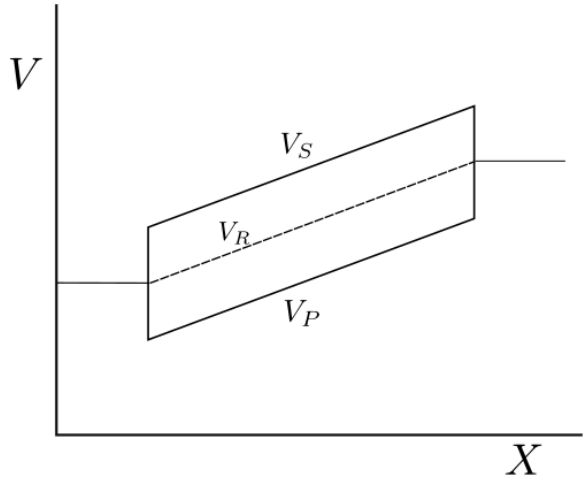

Fig. 2: Simplified velocity distributions of the turbine blades.

determine the displacement and momentum thicknesses. In this analysis, for the case of laminar flow, the Falkner-Skan velocity profiles are solved for each pressure gradient encountered [4]. For turbulent flow, the following equations are used [3].

$$\delta^*(x) = \frac{0.0463x}{Re_x^{1/5}} \qquad \theta(x) = \frac{0.036x}{Re_x^{1/5}} \qquad (3)$$

The same equations were used for both favorable and zero-pressure gradient flows, as the state of the boundary layer does not differ too significantly between the two [5].

Boundary Layer Losses

The entropic change due to profile loss in the boundary layer is expressed non-dimensionally with the viscous dissipation coefficient [2].

$$C_d = \frac{T\dot{S}}{\rho V^3} \qquad (4)$$

The value of C_d is modeled as a function of the Reynolds number based on momentum thickness. For constant pressure turbulent flow,

$$C_d = 0.0056\, Re_\theta^{-1/6} \qquad (5)$$

For accelerating turbulent boundary layers, simulations by Cebeci [6] show that the dissipation coefficient can be significantly less. Using a curve fit, the dissipation coefficient is modeled as

$$C_d = 0.0205\, Re_\theta^{-0.417} \qquad (6)$$

For laminar flows, the Pohlhausen family of velocity profiles can be integrated to attain dissipation coefficients [7].

$$C_d = \beta Re_\theta^{-1} \qquad (7)$$

The value of β ranges from 0.220 for highly favorable pressure gradients to 0.173 for constant pressure flows. The various values of C_d for turbulent, laminar, favorable, and zero pressure gradient boundary layers are plotted in Fig. 3. Clearly, the entropy

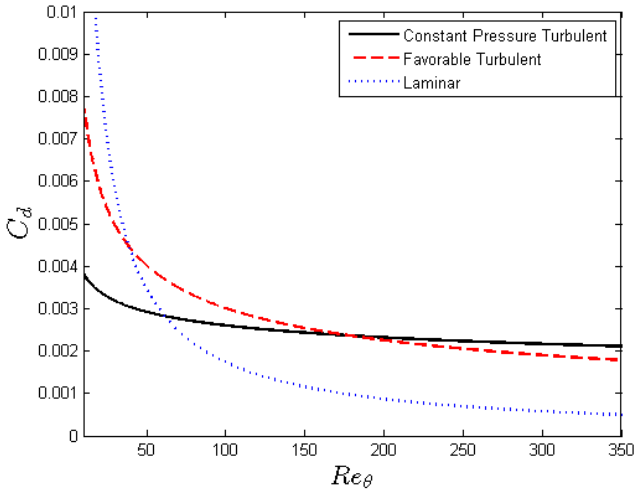

Fig. 3: Dissipation coefficient for various boundary layers.

generation in a laminar boundary layer is significantly less than its turbulent value near the transition point, highlighting the importance of maintaining a laminar boundary layer. In the present analysis, a value of $Re_\theta = 200$ was chosen as the transition point [3].

After determining the value of C_d over the blade, the total entropy generation per unit height within the boundary layer up to the trailing edge can then be computed for both the suction and pressure surfaces.

$$\dot{S} = \sum C \int_0^1 \frac{C_d \rho V^3}{T} d(x/C) \quad (8)$$

The summation occurs over all of the blades.

Trailing Edge Losses

Entropy is also created in the wake of the blade trailing edges, see Fig. 4. Three sources contribute to this entropy

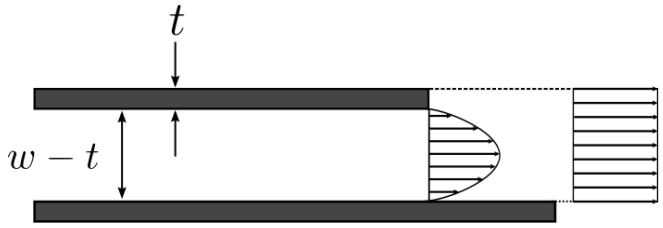

Fig. 4: Trailing edge of a turbine blade.

creation: the mixing out of the boundary layers at the trailing edge, a lower base pressure than would exist in an inviscid fluid, and the combined blockage from the boundary layers and the trailing edge itself. These loss mechanisms are analogous to the losses associated with a dump diffuser as described in Greitzer [3]. Denton combines these three loss sources into a loss coefficient.

$$\zeta = -\frac{C_{PB} t}{w} + \frac{2\theta}{w} + \left(\frac{\delta^* + t}{w}\right)^2 \quad (9)$$

For micro-turbomachinery, these losses can be significant. The trailing edge is thicker relative to the blade chord due manufacturing and stress constraints when compared to conventionally sized machines [1][8]. The growth rates for the boundary layer thickness parameters are also large relative to small chord lengths, as compared to larger machines.

Tip Clearance Losses

Entropy is generated as the lower velocity, higher pressure gas from the pressure side of the turbine blade spills over and mixes with the higher velocity gas stream of the suction surface, see Fig. 5. Shapiro [9] shows that the entropy creation from the injection of a small gas jet into a large gas stream is

$$\frac{ds}{c_p} = -2\frac{V_P}{V_S}\frac{(k-1)M^2}{2}\frac{dm}{m} + (k-1)M^2\frac{dm}{m} \quad (10)$$

After substituting in thermodynamic identities, this equation can be rearranged to give

$$Tds = \frac{1}{m}\int_0^C V_S^2 \left(1 - \frac{V_P}{V_S}\right) dm \quad (11)$$

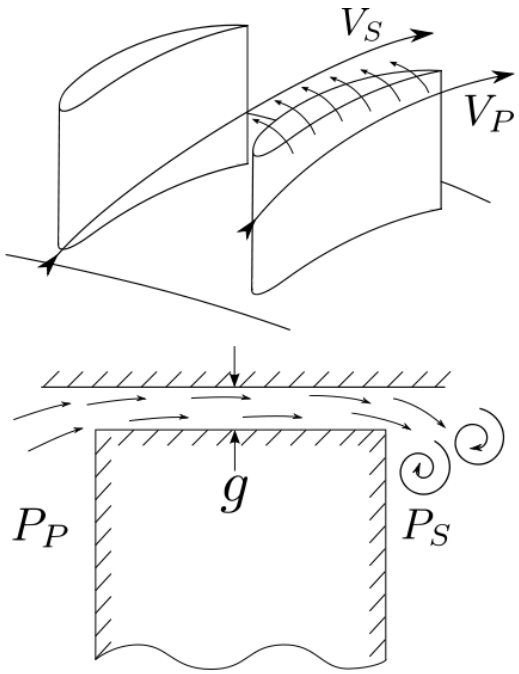

Fig. 5: Schematic of tip leakage.

The differential mass flow across the tip gap can be approximated with incompressible assumptions as a discharge flow through a clearance gap.

$$dm = C_{dis} g \sqrt{2\rho * \left[\frac{1}{2}\rho(V_S^2 - V_P^2)\right]}\, dC \quad (12)$$

C_{dis} is the discharge coefficient, chosen as 0.6 for this analysis, and g is the tip gap height. Equations 11 and 12 are combined to give the entropy creation from the tip leakage mixing process. Assuming the discharge coefficient does not vary significantly with gap height, the physics of this loss mechanism does not scale with size. However, due manufacturing constraints and rotational tolerances, the tip gap of micro-turbines is often constrained to be larger than in conventional devices [1].

RESULTS AND DISCUSSION

The entropy generation and associated power loss for each mechanism are numerically computed for single-stage, two-stage, and three-stage impulse turbines as well as a single-stage reaction turbine. The pitch to chord ratio was numerically cycled across a range of values in order to minimize the combined losses. These results are presented in Fig. 6. As expected, the best performing device is the single stage 50% reaction turbine, highlighting the advantage of favorable pressure gradients throughout the blade passages. An important observation is that because the losses per stage increase as diameter decreases, adding stages is more detrimental for microturbines than for conventionally sized machines, reducing the usefulness of this technique at the MEMS scale. In addition, the low efficiency results suggest that radial turbo-machinery should be pursued at small sizes, because the energy transfer due to centrifugal effects is

not subject to loss [10].

Lastly, the power density associated with each configuration was mapped over various diameters at their optimal rotor speed. The power density curve for a 50% reaction turbine is shown in Fig. 7. As shown, the power density increases over a large diameter range as expected from the squared-cubed law. However, at very small scales, the increased losses outweigh the benefits from the squared-cubed law and result in a diminished power density.

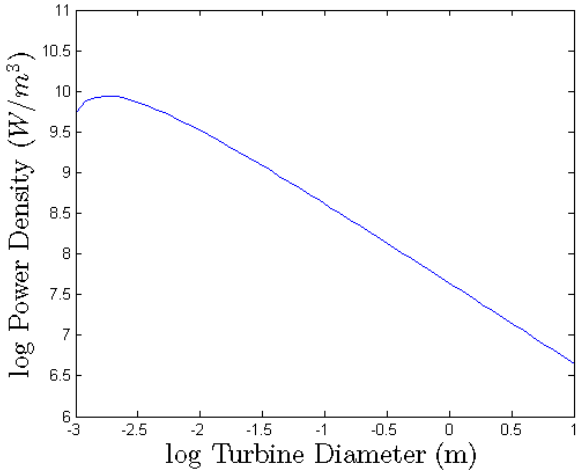

Fig 7. Power density of a single stage reaction turbine at optimal RPM as a function of diameter

REFERENCES

[1] C. Lee, S. Arslan, and L.G. Fréchette. Design principles of multistage radial flow microturbomachinery at low Reynolds numbers. Journal of Fluids Engineering , 130(11), 2008

[2] J.D. Denton. Loss mechanisms in turbomachines. Journal of Turbomachinery. 115:621-656, 1993

[3] E.M. Greitzer, C.S. Tan, and M.B. Graf, 2004. Internal Flows: Concepts and Applications. (Cambridge, Cambridge University Press)

[4] Cebeci, T., and Bradshaw 1977 Momentum Transfer in Boundary Layers (New York, McGraw-Hill Book Company)

[5] White, F.M., 1991 Viscous Fluid Flow (New York, McGraw-Book Company)

[6] Cebeci, T., and Carr, L.W, 1978. A Computer Program for calculating laminar and turbulent boundary layers for two-dimensional time-dependent flows. Tech. Rep. TM-78470, NASA

[7] Schlichting, H., 1968 Boundary-Layer Theory, 6th ed. (New York, McGraw-Hill Book Company)

[8] Osipov, I.L., 2008. A choice of trailing edge diameter of gas turbine blades. Thermal Engineering, 55(5), pg. 438-441

[9] Shapiro, A.H., 1953. The Dynamics and Thermodynamics of Compressible Fluid Flow, Vol. 1. (New York, The Roland Press Company)

[10] Cumpsty, N.A., 2004. Compressor Aerodynamics (Malabar, Krieger Publishing Company)

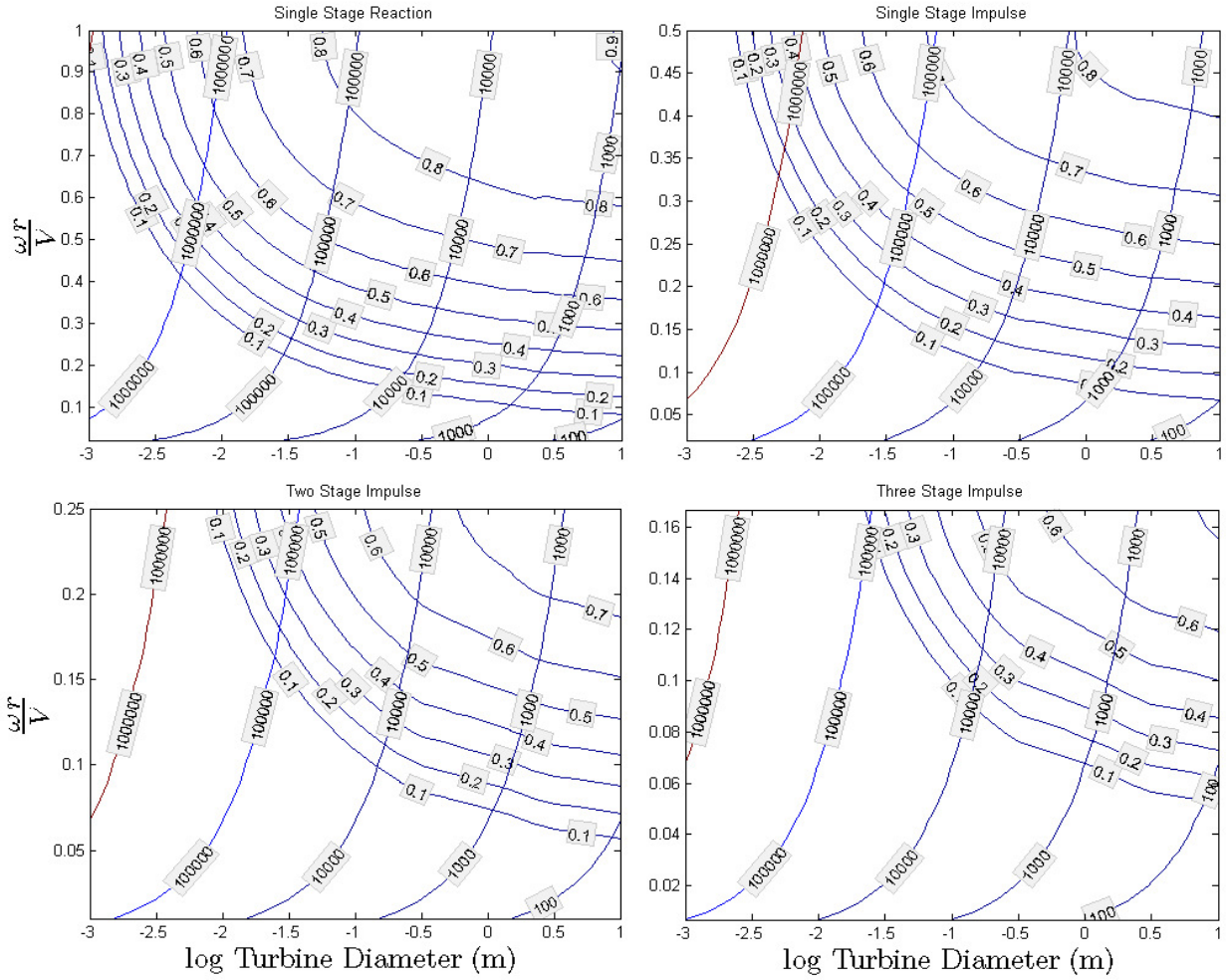

Fig. 6: Total-to-static efficiency of various turbines as a function of the velocity ratio, diameter, and RPM.